Photodegradation of methyl red under visible light by mesoporous carbon nitride

Yueyue Hu, Min Zhang, Zaozao Xiao, Tao Jiang, Bing Yan and Jian Li[1]

College of Chemical Engineering and Materials Science, Tianjin University of Science and Technology, Tianjin 300457, China

[1] lijian@tust.edu.cn

Abstract. Mesoporous carbon nitride (mpg-C_3N_4) with tunable microstructure has been successfully prepared through a simple polymerization reaction of cyanamide by a nano hard-templating approach. The obtained materials have been characterized using X-ray diffraction (XRD), N_2 adsorption, and Fourier transform infrared (FT-IR) spectroscopy. The results show that the pore diameter of the mpg-C_3N_4 materials can be easily tuned from 3.8 to 10.5 nm. The mpg-C_3N_4 materials are demonstrated to exhibit much higher visible light photocatalytic activity than that of g-C_3N_4 for the degradation of aqueous methyl red (MR). The high surface areas and large pore volume contributed to the efficient visible light photocatalytic activity.

1. Introduction

Dyes are considered as unpleasant and dangerous organic compounds for the environment. As reported by the Color Index (C.I.) which is managed by the Society of Dyers and Colorists (SDC) and the American Association of Textile Chemists and Colorists (AATCC), more than 100,000 different types of dyes are presently synthesized and are commercially available [1]. Although the exact amount of the worldwide dye production is not known, an annual production of over 700,000 tones has often been estimated [2]. Recent studies indicate that approximately 12% of the synthetic dyes are lost during the manufacturing and processing operations, about 20% of which enters the industrial wastewaters [3]. Dye-contaminated wastewater released to the environment causes numerous problems such as high chemical oxygen demand (COD), increase in toxicity [4] and a decrease in biodegradability [5, 6].

Azo dyes are the largest group of dyes used in industry. The term azo dye is applied to synthetic organic colorants that are characterized by a nitrogen-to-nitrogen double bond: -N=N- [7]. It is well known that methyl red (MR) dye has been used in paper printing and textile dyeing [8, 9] and it causes irritation of the eye, skin and digestive tract if inhaled/swallowed [10]. Methyl red (MR) with molecular formula $C_{15}H_{15}N_3O_2$ bearing an azo group is considered as carcinogenic. Student safety sheets for dyes and indicators classify MR as a harmful and irritating dye [11]. Therefore, once the water is contaminated with MR it is very difficult to remove it with traditional methods because some dyes are stable to light.

Thus, it is a great concern to remove MR from wastewater in an efficient and cost-effective way before its release to the environment. Many processes, such as incineration, biological treatment [12], ozonation, and solid phase adsorption, have extensively been used for the treatment of dye-bearing wastewater. However, these processes have their own limitations. The incineration can generate toxic volatile compounds; the biological treatment requires long time and, in many cases, leads to foul odor.

Moreover, in many cases, the process becomes unsuitable due to the resistance of the dye to biological degradation. Ozonation deals with ozone instability, and solid-phase adsorption results in toxic sludge.

Recently, photocatalytic degradation of organic pollutants by using nano-structured semiconductors [13, 14] offers great potential for the complete elimination of toxic chemicals. The g-C_3N_4 is an organic semiconductor [15] with medium bandgap of around 2.7 eV and is able to absorb visible light with bandgap absorption of 420-470 nm [16]. It has recently been reported to exhibit a good photocatalytic activity for hydrogen production [17] and organic degradation under visible light irradiation [18, 19]. However, C_3N_4 synthesized by self condensation of organic precursors is bulk material with a big sheet of lamellar structure and a very small surface area, normally below 10 m^2g^{-1} [19]. This fact makes it difficult to homogenously wrap around the photocatalysts and cannot provide more possible reaction sites for the catalytic reaction due to its small surface area [19, 20].

Compared to nonporous materials [21], mesoporous g-C_3N_4 (mpg-C_3N_4) feathers unique semiconductor properties along with an open crystalline pore wall and a large surface area facilitating mass transfer. The structure can in principle enhance the light harvesting ability and the reactant adsorption capability of the material due to its large surface and multiple scattering effects [19, 22].

In this study, mpg-C_3N_4 was synthesized by a hard-templating method using silica nanoparticles as the templates. The influences on the microstructure with different template/precursor ratios were studied. Metyl red (MR) was chosen as model pollutants in aqueous phase, and the polymeric catalysts were applied as metal-free photocatalysts under visible light illumination for MR degradation.

2. Experimental

2.1. Material

Cyanamide (CN-NH_2) was purchased from Rugao City Zhongru Chemical Co., Ltd, P. R. China. 40% dispersion of SiO_2 particles (particle diameter about 10 nm) was supplied by Beijing BOYU GOKE New Material Technology Co., Ltd, PR China. All other reagents used in this research were analytically pure and used without further purification.

2.2. Synthesis of mpg-C_3N_4

The mpg-C_3N_4 was synthesized with the hard template method as previously reported [14]. An amount of 4.5 g molten cyanamide was added dropwise in 22.5 g of a 40% dispersion of SiO_2 nanoparticles, which were used as a hard template. The mixture was heated at 90°C with stirring to evaporate water. The resultant white powder was then heated at a rate of 2.3°C min^{-1} over 4 h to reach a temperature of 550°C, and then tempered at this temperature for an additional 4 h. The brown-yellow product was treated with ammonium bifluoride (NH_4HF_2, 4 M) for 48 h to remove the silica template. The powders were then centrifuged and washed with distilled water for four times and with ethanol twice. Finally the mpg-C_3N_4 was dried at 70°C under vacuum for overnight, and defined as mpg-C_3N_4-0.5. A series of mpg-C_3N_4 photocatalysts with the different mass ratios of silica template to cyanamide were prepared by this method, which denoted as mpg-C_3N_4-r (r = 0.5, 1.5, 2.5). The bulk g-C_3N_4 was synthesized by directly heating 9 g of cyanamide at a rate of 2.3°C min^{-1} over 4 h to reach a temperature of 550°C, and then tempered at this temperature for an additional 4 h.

2.3. Characterization

X-ray diffraction (XRD) patterns of the powders were recorded at room temperature by a Shimadzu XRD-6100. Fourier transform infrared (FTIR) spectra were carried out using a Bruker spectrometer in the frequency range of 2000-600 cm^{-1} with a resolution of 4 cm^{-1}. The Brunauer-Emmett-Teller (BET) surface area was measured by Quantachrome Autosorb-iQ. The nitrogen adsorption and desorption isotherms were measured at 77 K after degassing the samples.

2.4. Photodegradation experiment

The photocatalytic activities were evaluated by the decomposition of Metyl red (MR) under visible light irradiation (>420 nm). Visible irradiation was obtained from a 500 W xenon lamp (Xujiang Electromechanical Plant, Nanjing, China) with a 420 nm cutoff filter. A certain amount of photocatalyst (25 mg) was totally dispersed in an aqueous solution of MR (50 mL, 0.01 mM). Before irradiation, the suspensions were magnetically stirred in the dark for 60 min to get absorption-desorption equilibrium between the photocatalyst and MR. At certain time intervals, 3 mL aliquots were sampled and centrifuged to remove the particles. The concentration of the MR was analyzed by a Hitachi U-3010 UV-vis spectrophotometer, and the original concentration of MR was defined as C_0. Before the absorbance measurements, the reaction solution was centrifuged for 10 min at 3000 r/min to remove the catalyst.

3. Results and discussion

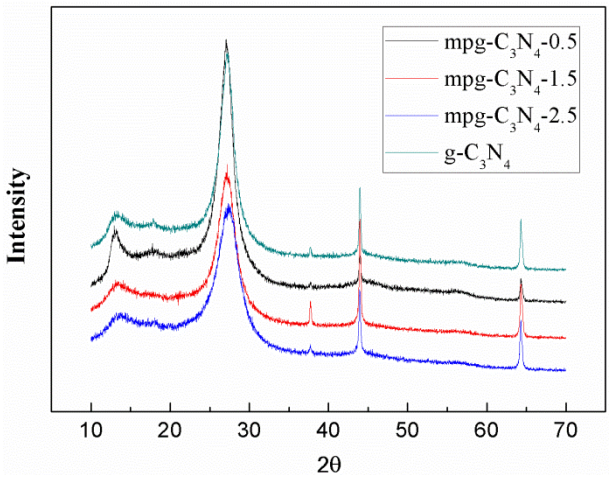

Figure 1. XRD patterns of bulk g-C_3N_4 and mpg-C_3N_4 samples.

Figure 1 shows the XRD pattern of the bulk g-C_3N_4 and mpg-C_3N_4-r synthesized at the temperature of 823 K. All of the samples had similar diffraction patterns as those seen in figure 1. A typical peak of approximately 27.6^o was indexed as (002) diffraction planes of C_3N_4 (JCPDS Card No. 87-1526), which indicates the graphite-like stacking of the conjugated aromatic units of CN with an interlayer distance of 0.33 nm [20]. The small additional peak at around 13.2^o, corresponding to interplanar distance of 0.67 nm, was indexed as (001) diffraction planes, which was associated with interlayer stacking [23]. Figure 1 also illustrates that the diffraction peak intensity weakens with increasing of r value. The decrease of the diffraction peak intensity implies that the crystallinity of the samples had been reduced.

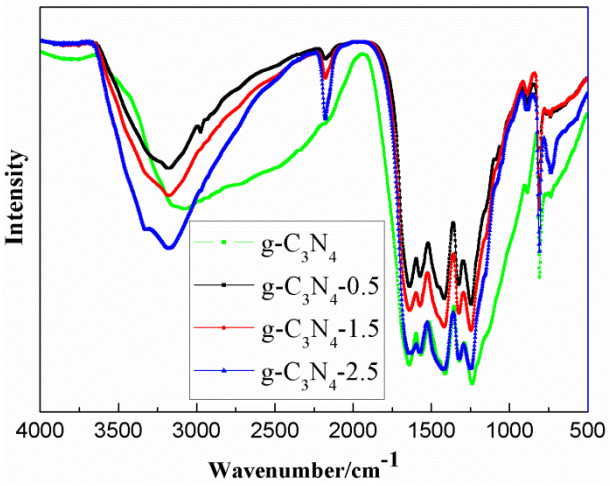

Figure 2. FTIR spectra of bulk g-C_3N_4 and mpg-C_3N_4 samples.

The surface functional groups of the carbon nitride materials were characterized by FT-IR and are shown in figure 2. The two bands at 1260 and 1610 cm^{-1} can be ascribed to aromatic C-N stretching bonds and aromatic ring modes, respectively. The weaker band at 3410 cm^{-1} may be related to the stretching mode of the NH groups in the aromatic ring. A shoulder at 1320 cm^{-1} is assigned to an sp3 C–C bond or disordered sp2 graphitic domains, and bands below 900 cm^{-1} are assigned to the graphitic sp2 domains. These results suggest that the mesoporous carbon nitrides are mainly composed of pyridine and benzene rings interconnected by nitrogen atoms [24].

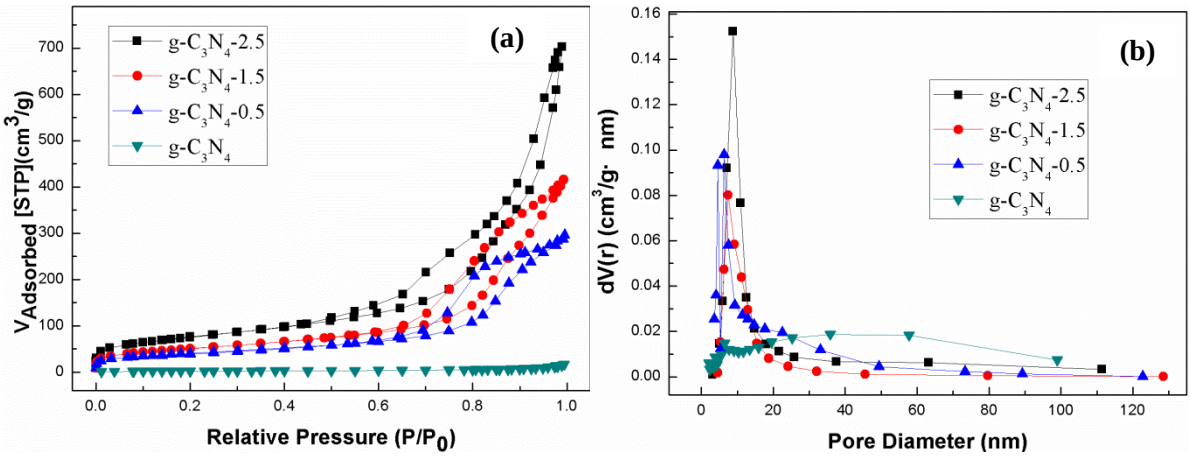

Figure 3. Nitrogen adsorption-desorption isotherms (a) and pore size distributions (b) of bulk g-C_3N_4 and mpg-C_3N_4 samples.

The nitrogen adsorption-desorption measurements performed at (-196 °C) for all examined samples (figure 3) demonstrated that textural characterizations of the used samples varied according to the quantity of nanosilica template. The g-C_3N_4 samples do not showed obviously hysteresis loop curves in figure 3a. However, for the mpg- C_3N_4 samples, the nitrogen adsorption-desorption isotherm followed the type IV according to the classification IUPAC, which is representative to the mesoporous materials [25]. The pore size distributions (figure 3b) were calculated by BJH method depending on the desorption branch. The pore diameter of mpg-C_3N_4 centered about 10 nm, which was agreement with the size of nanosilica template. The surface area of mesoporous samples is much higher than that of bulk material. mpg-C_3N_4-2.5 even presented a surface area as high as 267 m^2/g. The surface area and pore volume of mpg- C_3N_4 samples increase with the increasing amount of initial silica added, as

summarized in table 1. However, when the amount of silica further increases, we cannot obtain polymeric carbon nitride with an intact mesoporous structure.

Table 1. Physical properties of all bulk g-C_3N_4 and mpg-C_3N_4 samples.

Samples	S_{BET}(m^2/g)	Pore Volume(cm^3/g)	Diameter(nm)
g-C_3N_4	8.7	0.09	-
mpg-C_3N_4-0.5	147	0.42	9.50
mpg-C_3N_4-1.5	178	0.53	9.88
mpg-C_3N_4-2.5	267	0.73	10.46

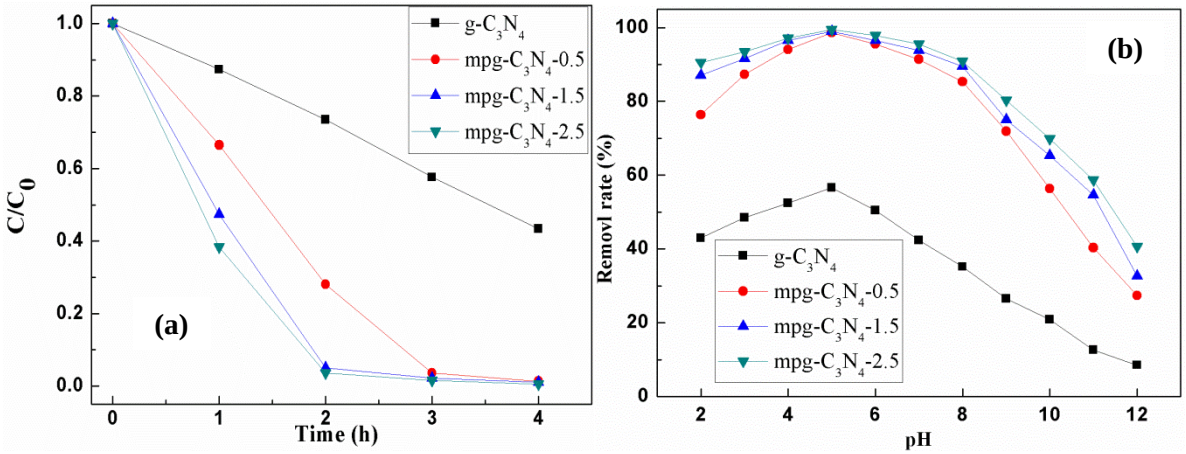

Figure 4. Visible-light photocatalytic degradation of MR over bulk g-C_3N_4 and mpg-C_3N_4 samples.

The photocatalytic degradation curves of MR as a function of reaction time are shown in figure 4a. The results illustrate that mesoporous structure greatly influences the photocatalytic performance of g-C_3N_4 materials. Bulk g-C_3N_4 shows a moderate photoreactivity toward the degradation of the pollutants. Only 18.3% of MR was degraded in 120 min over bulk g-C_3N_4 under visible light irradiation, and 42.4% was degraded in 240 min, which is however much smaller than those of mesoporous samples. mpg-C_3N_4-0.5 exhibits the higher photocatalytic activity, degrading nearly 72% of MR in 120 and 96% in 180 min, respectively. The catalytic activity of mpg-C_3N_4-1.6 and mpg-C_3N_4-2.5 was even much higher. More than 98% MR was degradated in 2h. This enlarged surface area of mpg- C_3N_4 not only facilitates the mass transfer of reaction species and the light harvesting by the multiple scattering effect of nanopores, but also provides more catalytic active sites for photoredox reaction. Thus, a better photocatalytic activity can be envisaged for mpg- C_3N_4 over bulk g-C_3N_4.

The initial dye concentration and reaction time were kept constant, while the pH was varied in order to investigate the effect of pH on the removal efficiency of MR.The removal of MR under different pH by g-C_3N_4, mpg-C_3N_4-0.5, mpg-C_3N_4-1.5 and mpg-C_3N_4-2.5 is presented in figure 4b. mpg-C_3N_4-2.5 exhibited superior performance compared to the other samples in a pH of range 2.0-7.0. The removal efficiency of all the flocculents was around 100% at a pH of 5.0. As previous research, mpg-C_3N_4 was positively charged under the test pH conditions, due to its -NH_2/-NH_3^+ pairs which are distributed on the edge of mesopores. Thus, the above improvement could be attributed to the increasing positive charge, which enhanced its neutralization ability [26]. The g-C_3N_4 removal efficiency was inferior to other samples in this case, and this can be attributed to the lower basicity of g-C_3N_4. The removal of anionic MR decreased as the pH increasing from 7.0 to 12.0 because higher concentration of OH^- ions reduce the positive charge of C_3N_4 and enhance the negative charge of MR,

which weaken the electrostatic attraction between catalyst and substrate. Thus, the concentration of MR in the mesopores was lower.

Acknowledgement
The authors thank the financial support from the National Natural Science Foundation of China (21306139, 21606172), the Project from Tianjin Education Commission (2017KDYB17, 2017KDYB18) and the Project (2015LG07,2014CXLG15) from Tianjin University of Science &Technology.

References

[1] Zollinger H 1987 In: Color Chemistry: Synthesis, Properties and Applications of Organic Dyes and Pigments (New York: VCH Publishers) pp 92–100
[2] McMullan G, Meehan C, Conneely A, Kirby N, Robinson T, Nigam P, Banat I M, Marchant R and Smyth W F 2001 Microbial decolourisation and degradation of textile dyes *Appl. Microbiol. Biotechnol.* **56** 81–87
[3] Hema M and Arivoli S 2007 Comparative study on the adsorption kinetics and thermodynamics of dyes onto acid activated low cost carbon *Int. J. Phys. Sci.* **2** 10–17
[4] Mohammed M A, Shitu A and Ibrahim A 2014 Removal of methylene blue using lowcost adsorbent: a review *Res. J. Chem. Sci.* **4**(1) 91–102
[5] Zhang C, Zhu Z, Zhang H and Hu Z 2012 Rapid decolorization of acid orange II aqueous solution by amorphous zero-valent iron *J. Environ. Sci.* **24**(6) 1021–26
[6] Wang Y, Gao B, Yue Q and Wang Y 2011 Effect of viscosity, basicity and organic content of composite flocculant on the decolourization performance andmechanism for reactive dyeing wastewater *J. Environ.Sci.* **23** 1626–33
[7] Student Safety Sheets 2007 Dyes & Indicators ©CLEAPSS
[8] Ghaedi M, Najibi A, Hossainian H, Shokrollahi A and Soylak M 2012 *Toxicol. Environ. Chem.* **9422** 40–48
[9] Sahoo C, Gupta A K and Anjali P 2005 1 *Desalination* **181** 91–100
[10] Lachheb H, Puzenat E, Houas A, Mohamed Ksibi, Elaloui E, Guillard C and Herrmann *J M Appl. Catal.* B **39** 75–90
[11] Badr Y, Abdul El-Wahed M G and Mahmoud M A 2008 *J. Hazard. Mater.* **154** 245–253
[12] Kumar G, Bakonyi P, Kobayashi T, Xu K, Sivagurunathan P, Kim S H, Buitrón G, Nemestóthy N, Bélafi-Bakó K 2016 Enhancement of biofuel production via microbial augmentation: The case of dark fermentative hydrogen *Renew. Sust. Energy Rev.* **57** 584–601
[13] Pan H, Gu B, Zhang Z 2009 Phase-dependent photocatalytic ability of TiO_2: a first-principles study *J. Chem. Theory Comput.* **5** 3074-78
[14] Dodouche I, Barbosa D P, Carmo Rangel M, Epron F 2009 Palladium–tin catalysts on conducting polymers for nitrate removal *Applied Catalysis B: Environmental.* **93** 50–55
[15] Pan H, Zhang Y, Shenoy V B, Gao H 2011 Ab initio study on a novel photocatalyst: functionalized graphitic carbon nitride nanotube *ACS Catal.***1** 99–104
[16] Zhao Z, Sun Y and Dong F 2015 Graphitic carbon nitride based nanocomposites: A review *Nanoscale*. **7** 15–37
[17] Shao M, Chai J, Qu Y, Yang M, Shi X, Wang S, Pan H 2017 Synergistic effect of 2D Ti_2C and g-C_3N_4 for efficient photocatalytic hydrogen production *J. Mater. Chem.* A. **5** 16748–56
[18] Zhang Y, Liu J, Wu G and Chen W 2012 Porous graphitic carbon nitride synthesized via directly polymerization of urea for efficient sunlight-driven photocatalytic hydrogen production *Nanoscale.* **4**(17) 5300
[19] Chen D, Wang K, Xiang D, Zong R, Yao W and Zhu Y 2014 Significantly enhancement of photocatalytic performances via core-shell structure of ZnO@mpg-C_3N_4 *Applied Catalysis B: Environmental* **147** 554–561
[20] Goettmann F, Fischer A, Antonietti M and Thomas A 2006 Chemical synthesis of mesoporous

carbon nitrides using hard templates and their use as a metal-free catalyst for Friedel-Crafts reaction of benzene, *Angew. Chem. Int. Ed.* **45** 4467–71

[21] Pan H, Zhang Y W 2012 GaN/ZnO superlattice nanowires as photocatalyst for hydrogen generation: A first-principles study on electronic and magnetic properties *Nano Energy* **1** 488–493

[22] Su F, Antoniettia M and Wang X 2012 mpg-C_3N_4 as a solid base catalyst for Knoevenagel condensations and transesterification reactions *Catal. Sci. Technol.* **2** 1005–09

[23] Talapaneni S N, Anandan S, Mane G P, Anand C, Dhawale D S, Varghese S, Mano A, Moricd T and Vinu A 2012 Facile synthesis and basic catalytic application of 3D mesoporous carbon nitride with a controllable bimodal distribution *J. Mater. Chem.* **22** 9831–40

[24] Shen W, Ren L, Zhou H, Zhang S and Fan W 2011 Facile one-pot synthesis of bimodal mesoporous carbon nitride and its function as a lipase immobilization support *J. Mater. Chem.* **21** 3890–94

[25] Sing K S W, Everett D H, Haul R A W, Moscou L, Pierotti R A, Rouquerol J and Sieminiewska T 1985 *Pure and Appl. Chem.* **57** 603–619

[26] Zhou W, Shen B, Meng F, Liu S and Zhang Y 2010 Coagulation enhancement of exopolysaccharide secreted by an Antarctic seaice bacterium on dye wastewater *Sep. Purif. Technol.* **76** 215–221